Supporting information

Synthesis and SMM Behaviour of Trinuclear versus Dinuclear 3d-5f Uranyl(V)-Cobalt(II) Cation-Cation Complexes.

Lucile Chatelain,[a] *Floriana Tuna*[b] *Jacques Pécaut*[c] *and Marinella Mazzanti**[a]

[a] EPFL, ISIC, Batiment CH J2 490, 1015 Lausanne, Switzerland

[b]School of Chemistry and Photon Science Institute, University of Manchester, Oxford Road, Manchester, M13 9PL, United Kingdom

[c]Laboratoire de Reconnaissance Ionique et Chimie de Coordination, SCIB, UMR-E3 CEA-UJF , INAC, CEA-Grenoble, 17 rue des Martyrs, F-38054 Grenoble Cedex 09, France.

E-mail: marinella.mazzanti@epfl.ch

*Correspondence to Dr. Marinella Mazzanti

Table of Contents

1. General considerations

All manipulations were carried out under an inert argon atmosphere using Schlenk techniques and an MBraun glovebox equipped with a purifier unit. The water and oxygen level were always kept at less than 1 ppm. The solvents were purchased from Aldrich in their anhydrous form conditioned under argon and were vacuum distilled from K/benzophenone (hexane, pyridine) or CaH_2 (MeCN). Depleted uranium turnings were purchased from the "Société Industrielle du Combustible Nucléaire" of Annecy (France). Anhydrous CoI_2 salt was purchased from Aldrich and was used without further purification. TPA and BPPAH ligands were prepared as previously described.[1] $[UO_2(\mathrm{Mesaldien})K]_\infty$ (Mesaldien=N,N'-(2-aminomethyl)diethylenebis(salicylidene imine)) was synthesized as previously described.[2] Elemental analyses were performed under argon by Analytische Laboratorien GMBH at Lindlar, Germany.

Caution: Depleted uranium (primary isotope ^{238}U) is a weak α-emitter (4.197 MeV) with a half-life of 4.47×10^9 years. Manipulations and reactions should be carried out in monitored fume hoods or in an inert atmosphere glovebox in a radiation laboratory equipped with α- and β-counting equipment.

2. Synthesis

2.1. Synthesis of {[Co(TPA)][UO$_2$(Mesaldien)]}I, 1

To a dark blue solution of [UO$_2$(Mesaldien)K]$_\infty$ (87.1 mg, 0.138 mmol, 1 eq.) in 2 mL of pyridine is added a blue solution of [Co(TPA)I]I prepared *in situ* from the reaction of CoI$_2$ (41.5 mg, 0.138 mmol, 1 eq.) and TPA (38.6 mg, 0.138 mmol, 1 eq.) in 1 mL of pyridine. Immediately the color changes to dark violet and a violet solid precipitates out of the solution. The resulting suspension is stirred at room temperature for 3 hours before filtration of the violet solid, which is washed with 2*0.5mL of pyridine and dried under reduced pressure yielding 82.9 mg of **1**. Another portion of **1** is obtained by slow diffusion of hexane in the violet filtrate yielding 25.6 mg more of **1** (0.100 mmol, 73%). Dark violet X-ray quality crystals of **1**.Pyridine were formed after two weeks at room temperature from a solution of **1** in pyridine layered with hexane. ^{1}H NMR (400 MHz, CD$_3$CN, 298 K): δ = 138.39 (br, 4H), 97.45 (br, 6H), 50.89 (s, 2H), 46.64 (s, 2H), 17.36 (s, 2H), 12.91 (s, 2H), 9.74 (s, 2H), 8.12 (s, 2H), 6.39 (s, 2H), 5.62 (s, 2H), 4.66 (s, 2H), 3.98 (s, 2H), 3.64 (s, 2H), 0.30 (s, 2H), -0.84 (s, 2H), -1.22 (br, 3H). ESI-MS : m/z=942.1 ({[Co(TPA)][UO$_2$(Mesaldien)]}$^+$). Elemental analysis (%) calculated for [UO$_2$(Mesaldien)][Co(TPA)]}I.0.1Pyridine (C$_{37.5}$H$_{39.5}$N$_{7.1}$O$_4$CoIU MW=1077.53) C 41.80, H 3.70 and N 9.23 found C 41.79, H 3.77 and N 9.30.

2.2. Synthesis of {[Co(BPPA)][UO$_2$(Mesaldien)][Co(BPPA)(Py)]}I, 2

A brown suspension of [Co(BPPA)I] prepared *in situ* from the reaction of CoI$_2$ (52.4 mg, 0.167 mmol, 2 eq.) and BPPAK (57.5 mg, 0.167 mmol, 2 eq.) in 1 mL of pyridine is added to a stirred dark blue solution of [UO$_2$(Mesaldien)K]$_\infty$ (0.34THF) (55 mg, 0.084 mmol, 1 eq.) in 2 mL of pyridine. Immediately the resulting solution turned dark red. After 3 hours of stirring, KI was filtrated off and the solution was layered with hexane. Dark X-ray quality crystals of **2**.2.5Pyridine were formed after two weeks. Crystals were collected by filtration and washed with hexane (2 x 0.5 mL) and dried under vacuum to yield 130.1 mg of {[Co(BPPA)][UO$_2$(Mesaldien)][Co(BPPA)(Py)]}I.2Pyridine (0.077 mmol, 92%). ^{1}H NMR (200 MHz, CD$_3$CN, 298 K): δ = 145.49 (br, 3H), 134.36 (br, 4H), 101.733 (br, 2H), 70.03 (br, 3H), 60.39 (br, 1H), 51.44 (s, 4H), 40.4 (d, 4H), 35.00 (br, 2H), 25.34/24.47 (br m, 2H), 13.30 (br, 2H), 7.94 (d, 4H), 6.24 (s, 2H), 5.39 (s, 2H).4.65 (s, 2H), 4.39 (s, 2H), 4.11 (s, 2H), 3.63 (s, 2H), 1.43 (br, 2H), -0.16/-0.69 (br m, 5H), -15.35 (br, 2H), -19.39 (br, 2H). ESI-MS : m/z=1319.2 ({[Co(BPPA)][UO$_2$(Mesaldien)][Co(BPPA)]}$^+$). Elemental analysis calcd (%) for **2**.2py, {[Co(BPPA)(Py)][UO$_2$(Mesaldien)][Co(BPPA)]}I.2Pyridine (C$_{72}$H$_{72}$N$_{12}$O$_6$ICo$_2$U MW=1684.04) C 51.35, H 4.31 and N 9.98; found C 51.33, H 4.16 and N 10.33.

3. X-ray crystallography.

Diffraction data were taken using an Oxford-Diffraction XCallibur S kappa geometry diffractometer (Mo-Kα radiation, graphite monochromator, $\lambda = 0.71073$ Å). To prevent evaporation of co-crystallised solvent molecules the crystals were coated with light hydrocarbon oil and the data were collected at 150 K. The cell parameters were obtained with intensities detected on three batches of 5 frames. The crystal-detector distance was 4.5 cm. The number of settings and frames has been established taking in consideration the Laue symmetry of the cell by CrysAlisPro Oxford-diffraction software.[3]1108 for **1** narrow data were collected for 1° increments in ω with a 15 s exposure time. 267 for **2** narrow data were collected for 1° increments in ω with a 10 s exposure time. Unique intensities detected on all frames using the Oxford-diffraction Red program were used to refine the values of the cell parameters. The substantial redundancy in data allows analytical absorption correction for **1** and **2** Oxford-diffraction program. [3] Space groups were determined from systematic absences, and they were confirmed by the successful solution of the structure. The structures were solved by direct methods using the SHELXTL 6.14 package. [4] All non-hydrogen atoms were found by difference Fourier syntheses and refined on F^2. Hydrogen atoms were fixed in ideal position. Experimental details for X-ray data collections of **1** and **2** are given in Table S1. CCDC 1011215-1011216 contain the supplementary crystallographic data for this paper. These data can be obtained free of charge from The Crystallographic Data Centre via www.ccdc.cam.ac.uk/data_request/cif. Figure Graphics are generated using MERCURY 2.3 Supplied with Cambridge Structural Database; CCDC: Cambridge, U.K., 2004-2009.

X-ray quality crystals of **1**.1Py were obtained by slow diffusion of hexane into a pyridine solution of **1**.

Table S1. Crystallographic Data for Compounds **1** and **2**

	1·(C_5H_5N)	**2**·2.5(C_5H_5N)
Formula	$C_{42}H_{44}CoIN_8O_4U$	$C_{74.5}H_{74.5}ICo_2N_{12.5}O_6U$
Crystal size (mm)	0.92 x 0.12 x 0.09	0.373 x 0.316 x 0.197
cryst syst	Trigonal	Monoclinic
space group	R_{-3}	$I_{2/a}$
volume (Å^3)	19728.4(6)	15447(2)
a (Å)	43.0624(8)	31.576(2)
b (Å)	43.0624(8)	19.4882(11)
c (Å)	12.2847(2)	27.130(2)
α (deg)	90	90
β (deg)	90	112.290(9)
γ (deg)	120	90
Z	18	8
formula weight (g/mol)	1148.71	1723.75
density (g cm^{-3})	1.740	1.482
absorption coefficient (mm^{-1})	4.821	2.972
F(000)	10008	6848
temp (K)	150.0(2)	150.0(2)
total no. reflections	81984	48922
unique reflections [R(int)]	13354 [R(int) =	23483 [R(int) = 0.0964]
Final R indices [I > 2σ(I)]	R1 = 0.0428, wR2 =	R1 = 0.0864, wR2 =
Largest diff. peak and hole	4.798 and -2.425	2.260 and -1.356
GOF	1.080	1.011

Selected Intra- and inter-molecular Bond Distances

The intramolecular U–Co distance is 3.73882(5) Å. In **1** the shortest intermolecular U–U, U–Co and Co–Co distances are, respectively, 8.31382(13), 7.26841(12) and 8.14835(10) Å.

The mean intramolecular U-Co distance is 3.9068(2) Å whereas the Co-Co intramolecular distance is 7.8089(4) Å in **2**. Finally the shortest intermolecular U-U, U-Co and Co-Co distances are 10.4919(14), 9.7639(11) and 7.7742(7) Å in **2**.

4. NMR studies

^{1}H NMR spectra were recorded on Bruker 200 MHz and 400 MHz spectrometers. NMR chemical shifts are reported in ppm with solvent as internal reference.

4.1. NMR spectra

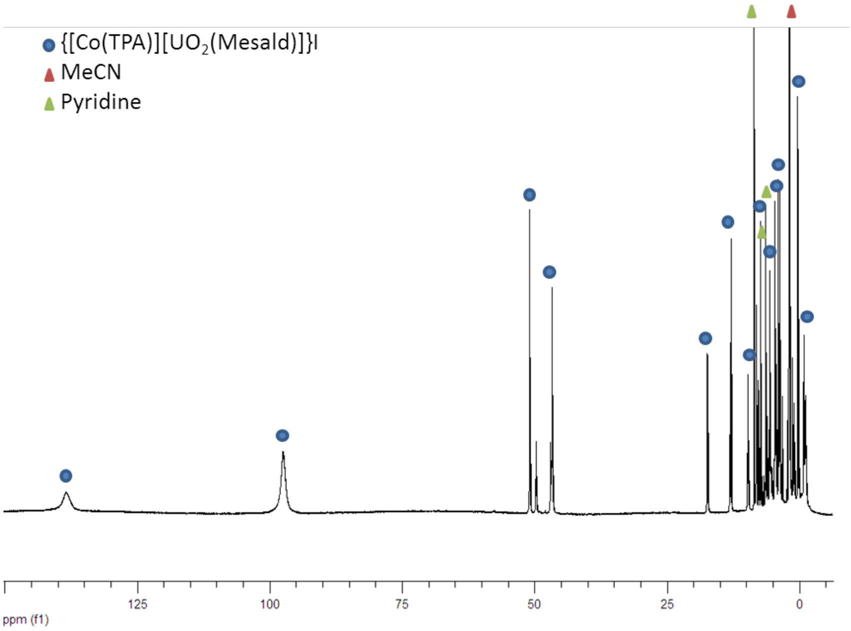

Figure S1. ^{1}H NMR (400MHz, CD_3CN, 298 K) of complex {[Co(TPA)][UO$_2$(Mesaldien)]}I.0.1Pyridine **1**.

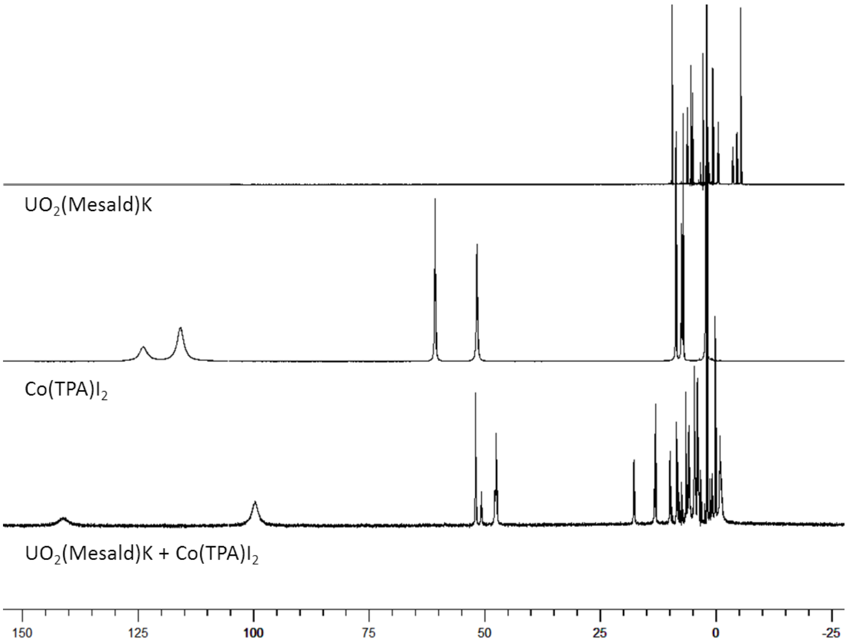

Figure S2. ^{1}H NMR (200MHz, CD_3CN, 298K) of complex {[Co(TPA)][UO$_2$(Mesaldien)]}I.0.1Pyridine **1**.0.1Pyridine compared to [Co(TPA)I]I and [UO$_2$(Mesaldien)K] complexes.

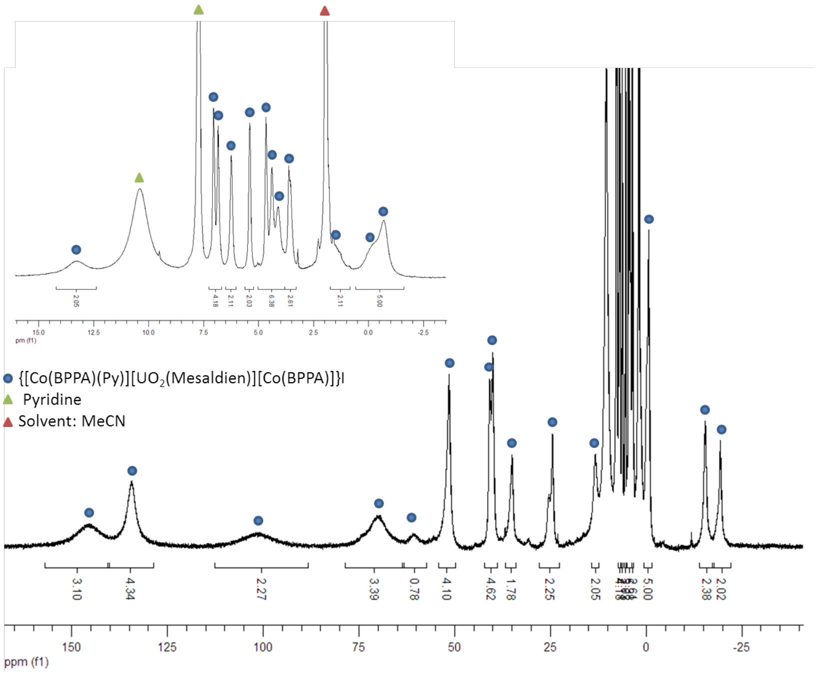

Figure S3. ^{1}H NMR (200 MHz, CD_3CN, 298 K) of complex {[Co(BPPA)][UO$_2$(Mesaldien)][Co(BPPA)(Py)]}I **2**.

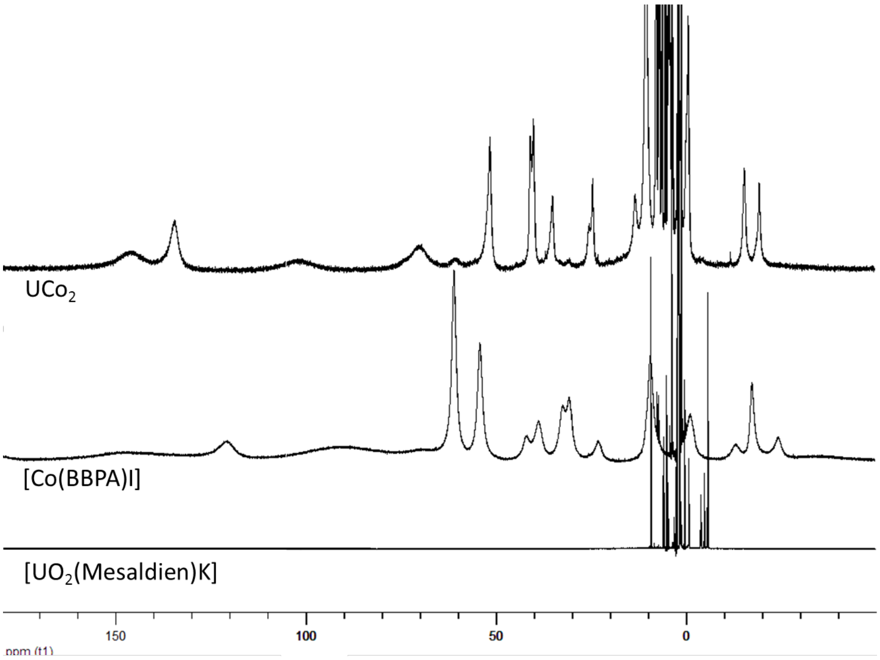

Figure S4. ^{1}H NMR (200MHz, CD_3CN, 298K) of complex {[Co(BPPA)][UO$_2$(Mesaldien)][Co(BPPA)(Py)]}I **2** compared to [Co(BPPA)I] and [UO$_2$(Mesaldien)K] complexes.

4.2. Spherical hydrodynamic radius

The diffusion NMR experiments were performed using a Pulsed-Field Gradient STimulated Echo (PFGSTE) sequence, using bipolar Gradients, at 298 K and no spinning was applied to the NMR tube. [5]The spherical hydrodynamic radius (called Stokes radius) of the molecule was calculated from the Stokes-Einstein equation and compared to the value obtained from the solid state structure and with a similar reference compound in the same solvent:

$$r_{sph} = \frac{k_B T}{6\pi\eta D}$$

η (Pa.s^{-1}) = viscosity of the medium, k_B (m².kg.s^{-2}.K^{-1}) = Boltzmann constant, T = absolute temperature (K), D = diffusion coefficient (m².s^{-1}).

Results:

The values of the diffusion coefficient obtained for **1** was compared with those measured for the monomeric [UO$^{VI}_2$(Mesaldien)] complex in the same solvent and at the same temperature. No diffusion coefficient has been obtained for **2** as the application of a gradient kills all the broad peaks.

Table S2. Diffusion Coefficient Values for **1** and Estimated Spherical Radii

acetonitrile η= 0.343 mPa.s (298 K)	**Diffusion coefficient (m².s^{-1})**	**Hydrodynamic radii**	**Radii evaluated from crystal**
[UO_2(Mesaldien)]	1.63 10^{-9}	3.9	3.59
{[Co(TPA)][UO_2(Mesaldien)]}.I	1.575 10^{-9}	4.0	4.4

5. Mass spectroscopy

Mass spectra were acquired on a LXQ-linear ion trap (Thermo Scientific, San Jose, CA,USA), equipped with an electrospray source in a pyridine/acetonitrile mixture (1:1 to 1:5) which was prepared and filtered on microporous filters in the glove-box and maintained under argon until injection in the spectrometer. Electrospray full scan spectra, in the range of *m/z* 50 –3000 amu, were obtained by infusion through fused silica tubing at 2-10 µL min^{-1}.

The LXQ calibration (*m/z* 50-2000) was achieved according to the standard calibration procedure from the manufacturer (mixture of caffeine/MRFA and Ultramark 1621). The LXQ calibration (*m/z* 2000-4000) was performed with ES tuning mix (Agilent). The temperature of the heated capillary of the LXQ was set to the range of 180-220 °C, the ion spray voltage was in the range of 1 – 3 kV with an injection time of 5-100 ms. The experimental isotopic profile was compared in each case to the theoretical one.

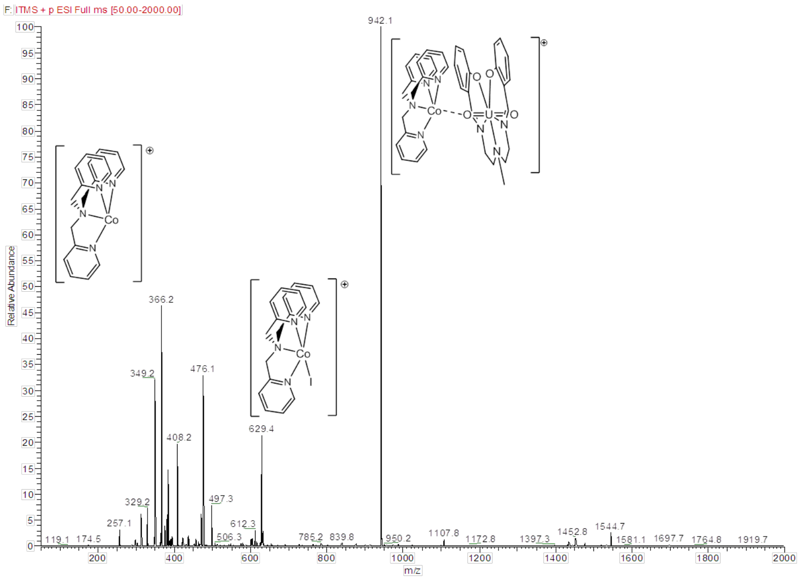

Figure S5. ESI/MS spectra of **1** in acetonitrile.

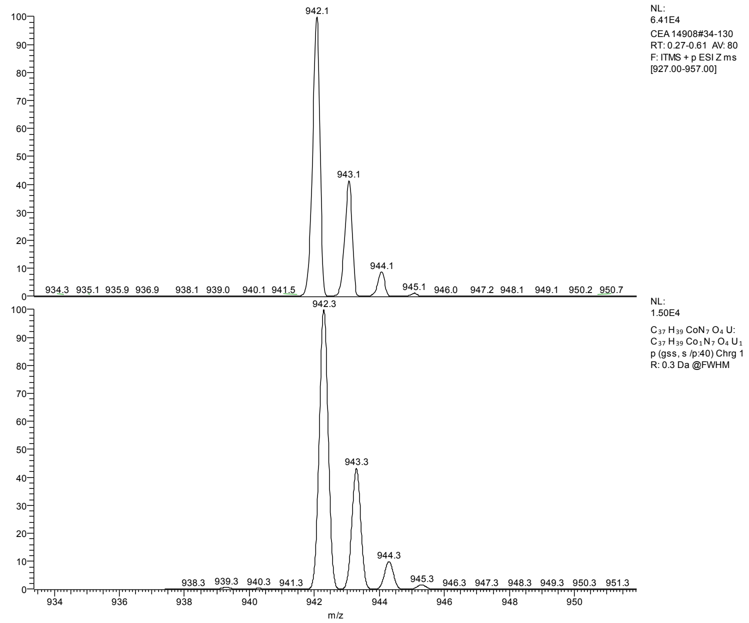

Figure S6. Zoom on the molecular peak (top) compared with the theoretical isotopic (bottom) profile calculated for $\{[Co(TPA)][UO_2(Mesaldien)]\}^+$.

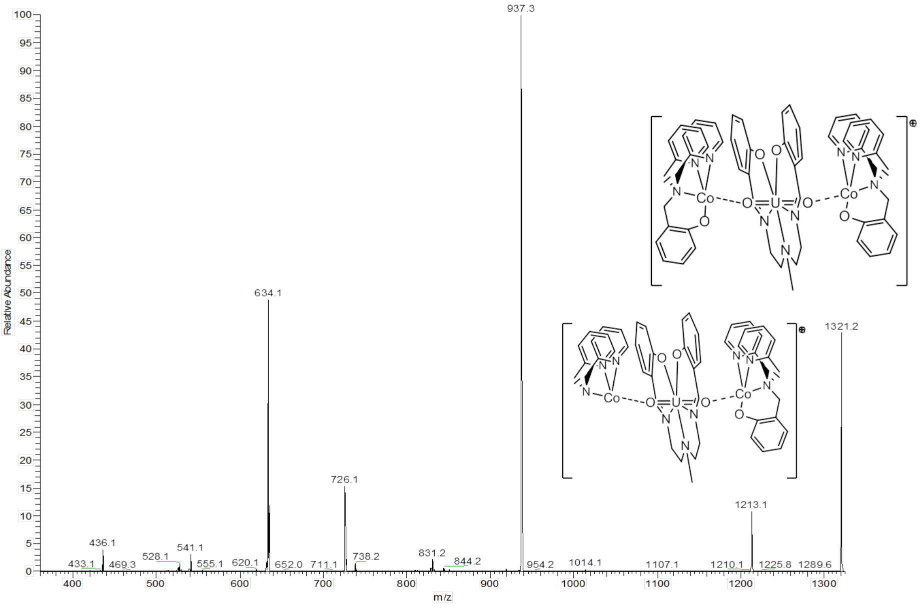

Figure S7. ESI/MS spectra of **2** in acetonitrile.

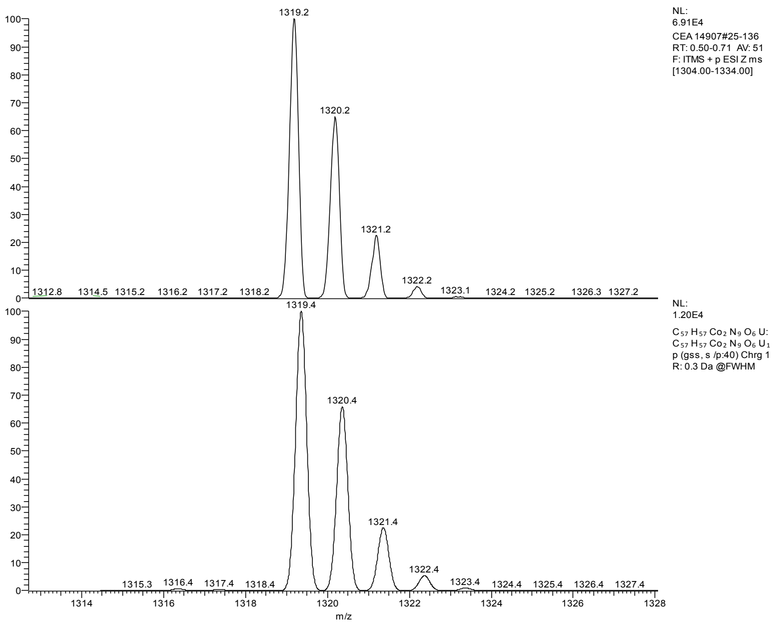

Figure S8. Zoom on the molecular peak (top) compared with the theoretical isotopic (bottom) profile calculated for {[Co(BBPA)][UO_2(Mesaldien)][Co(BBPA)]}$^+$.

6. Magnetic studies

Variable-temperature magnetic susceptibility and isothermal magnetisation versus field data were recorded in the temperature range 1.8–300 K with a Quantum Design MPMS-XL 7T and a Quantum Design MPMS-XL 5.0 Superconducting Quantum Interference Devices (SQUID). Measurements were carried out on finely ground polycrystalline samples of **1** and **2** restrained in eicosane (to prevent sample torqueing). Suprasil-Quartz tubes were used as sample holders and were sealed under vacuum before measurement. Reproducibility of the magnetic measurement was verified by the independent measurement of three samples from three different synthetic batches. The contribution to the signal of the empty sample holder was measured and subtracted from the total signal. Experimental data were further corrected for the diamagnetic contribution of the compounds using tabulated Pascal's constants. Magnetic calibration was performed using a cylindrical palladium standard having approximately the same geometry of the measured samples. Isothermal magnetization loops were measured while sweeping the magnetic field at a constant rate, from +7 to −7 T and back, with the sample fixed at temperatures ranging from 1.8 to 10 K. The real and imaginary components, χ' and χ'', of the complex ac magnetic susceptibility were measured as a function of temperature (1.8-10 K) and frequency (0.1 -1400 Hz) using a Quantum Design MPMS-XL 7T magnetometer. All ac measurements were performed under an oscillating field of 1.55 G.

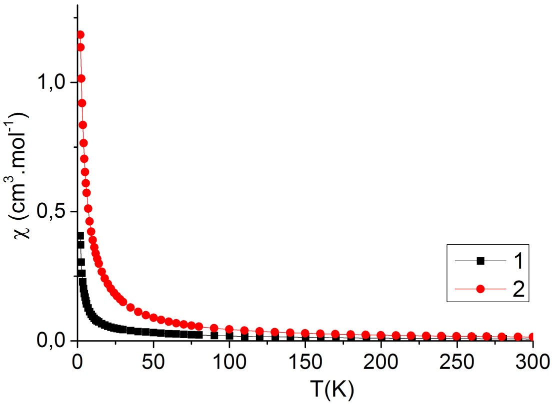

Figure S9. Temperature dependent of magnetic susceptibility data of **1**.0.1Pyridine and **2**.2Pyridine measured at fields of 0.5T recorded in the range 2–300 K {[UO_2(Mesaldien)][Co(TPA)]}I.0.1Pyridine (χ_{dia}=-4.86×10^{-4} emu.mol^{-1}, m=20.1 mg, M_r=1077.53 g.mol^{-1}) {[Co(BPPA)] [UO_2(Mesaldien)][Co(BPPA)(Py)]}I.2Pyridine χ_{dia}=-8.75×10^{-4} cm^3.mol^{-1}, m=23.2 mg, M_r=1723.19 g.mol^{-1}).

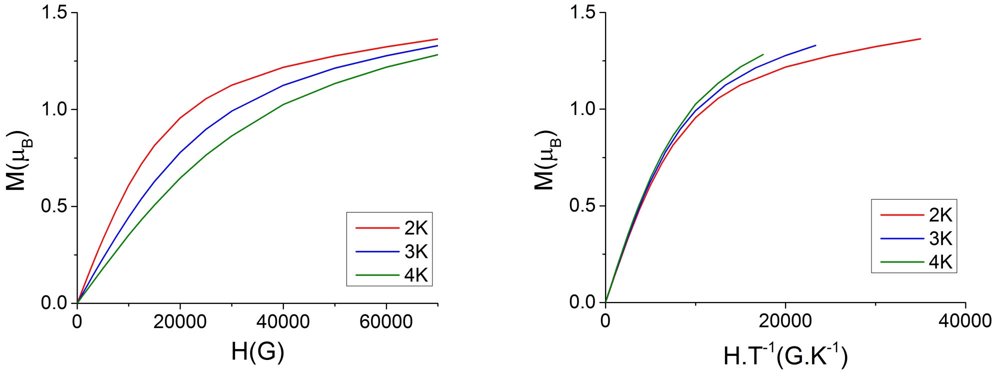

Figure S10. Plots of *M*(*H*) versus *H* (left) and *M*(*H*) versus *H*/*T* (right) for **1**.0.1Pyridine at several temperatures between 2 and 4 K.

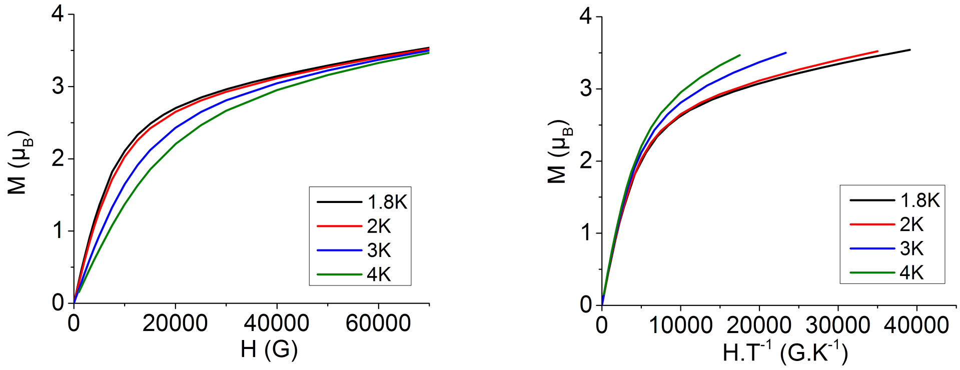

Figure S11. Plots of *M*(*H*) versus *H* (left) and *M*(*H*) versus *H*/*T* (right) for **2**.2Pyridine at several temperatures between 1.8 and 4 K.

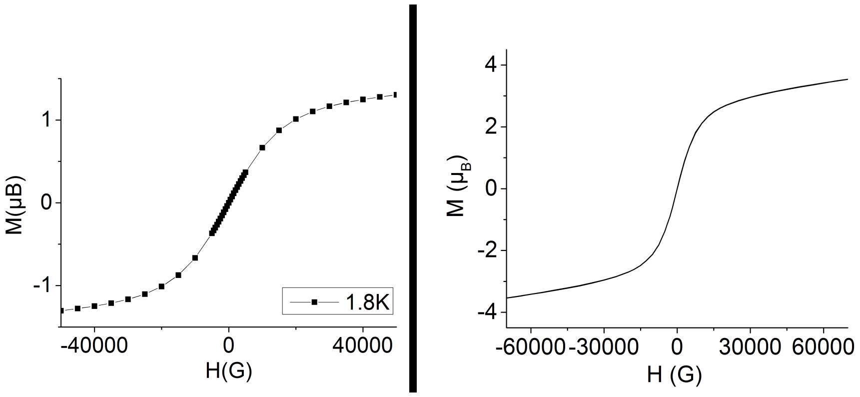

Figure S12. Magnetic hysteresis loops for a polycrystalline sample of **1**.0.1Pyridine (left) and **2**.2Pyridine (right) recorded at 1.8 K under the same field sweep rate of 0.0013 T/s.

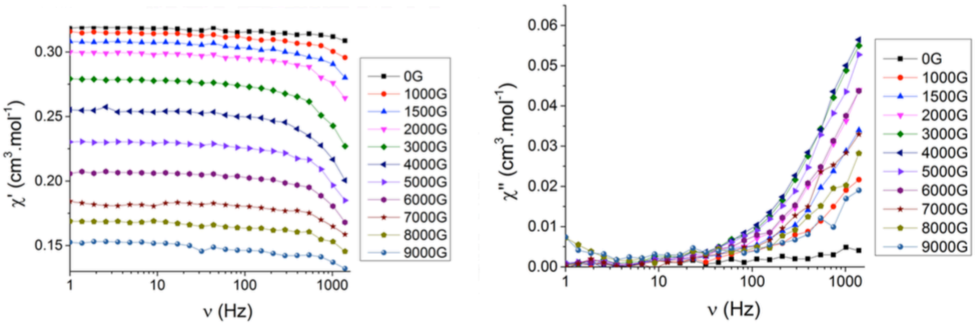

Figure S13. dc field dependencies at 1.8 K of the in-phase (left) and out-phase (right) ac susceptibility (χ'') plotted vs. ν(Hz) of **1**.0.1Pyridine recorded with an ac field of 1.55 Oe oscillating between 1 and 1400Hz.

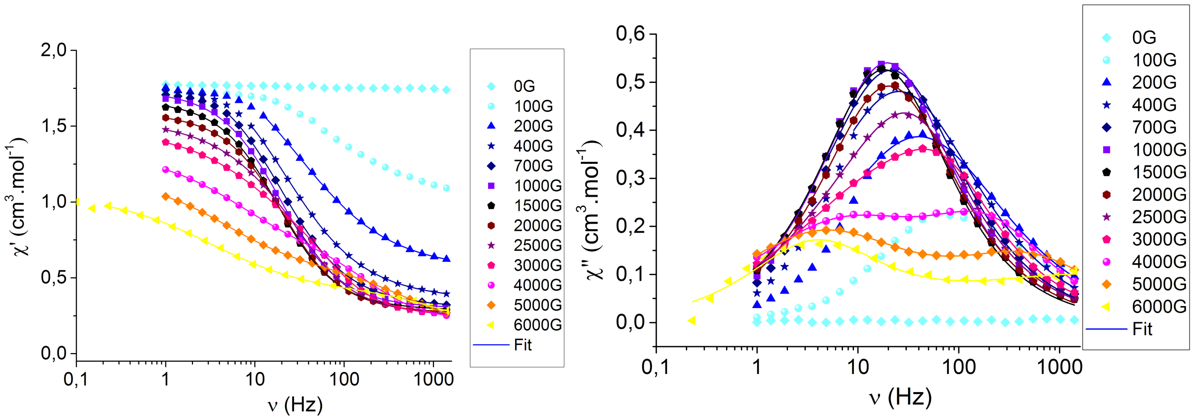

Figure S14. dc field dependencies at 1.8K of the in-phase (left) and out-phase(right) ac susceptibility (χ'') plotted vs. ν(Hz) of **2**.2Pyridine recorded with an ac field of 1.55 Oe oscillating.

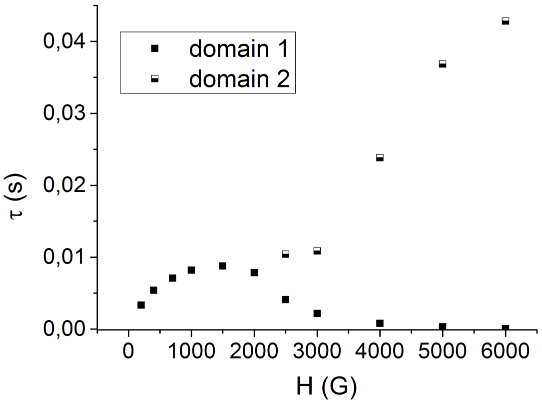

Figure S15. dc field dependency at 1.8K of the relaxation time revealing two relaxation processes for **2**.2Pyridine, at low and high field.

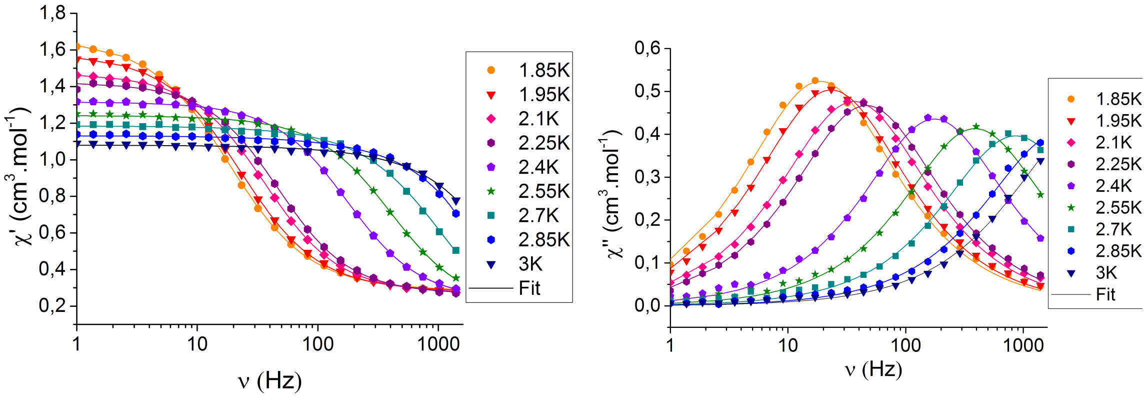

Figure S16. Frequency dependencies at 1500G dc field of the (left) in-phase and (right) out-of-phase ac susceptibility components of **2**.2Pyridine recorded at several temperatures between 1.85 and 3 K with an ac field of 1.55 Oe oscillating at frequencies between 1 and 1400 Hz. The straight lines represent the Debye fits to the experimental data. (Argand plots)

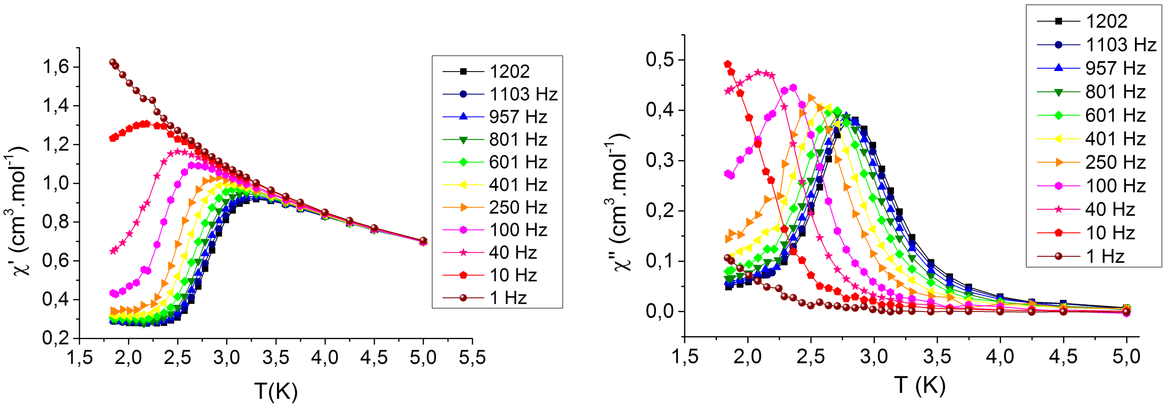

Figure S17. Temperature dependencies of the (left) real (χ') and (right) imaginary (χ'') ac. susceptibility for **2**.2Pyridine measured at 1500G dc field and 1.55 G ac field.

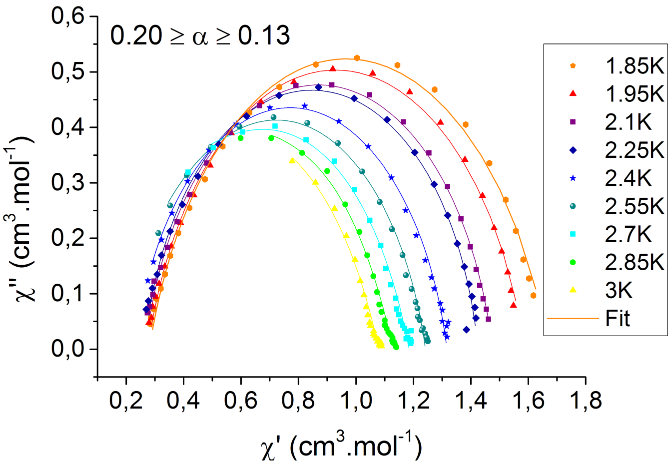

Figure S18. Cole-Cole plots and Debye fits (straight lines) (χ' and χ'' measured at 1500 G) for **2**.2Pyridine at several temperatures between 1.85 and 3 K. For the latter, semi-circular Cole–Cole plots (χ_M'' vs χ_M') were obtained at fixed temperatures between 1.85 and 2.7 K indicating the presence of a single relaxation process which could be fitted to a generalized Debye model with an α parameter in the range of 0.12–0.2; this is consistent with a narrow distribution of relaxation times.

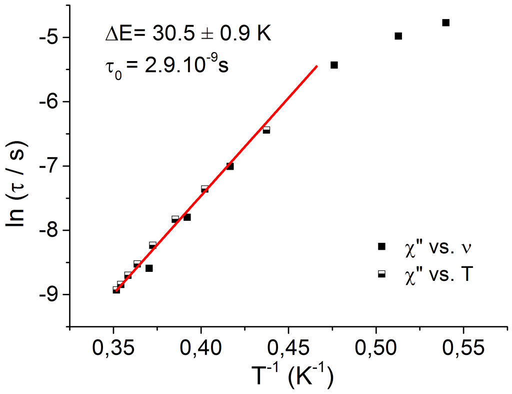

Figure S19. Arrhenius plot for **2**.2Pyridine based on relaxation times obtained from the ac data collected as a function of temperature (half open squares) and frequency (black squares). A linear fit gives a thermal relaxation barrier of 30.5 K ± 0.9 K and a relaxation rate of 2.9 x 10^{-9} s.

1. G. Anderegg and F. Wenk, *Helv. Chim. Acta*, 1967, **50**, 2330-2332.
2. V. Mougel, J. Pecaut and M. Mazzanti, *Chem. Commun.*, 2012, **48**, 868-870.
3. **C. R. CrysAlisPro CCD, ABSPACK, CrysAlis PRO. Agilent Technologies**, Agilent Yarnton, England, 2010.
4. G. M. Sheldrick, ed. B. A. Inc, Madison,Wisconsin, USA, 6.14 edn., 1997.
5. (a)J. E. Tanner, *J. Chem. Phys.*, 1970, **52**, 2523-&; (b)D. H. Wu, A. D. Chen and C. S. Johnson, *J. Magn. Reson., Series A*, 1995, **115**, 260-264; (c)C. S. Johnson, *Prog. Nucl. Magn. Reson. Spectrosc.*, 1999, **34**, 203-256.